

Bayesian Estimation of the Transmissivity Spatial Structure from Pumping  
Test Data

Mehmet Taner Demir<sup>1</sup>, Nadim K Coptý<sup>1</sup>, Paolo Trincherò<sup>2</sup>, Xavier Sanchez-Vila<sup>3</sup>

<sup>1</sup> Institute of Environmental Sciences, Bogazici University, Istanbul, 34342 Turkey

<sup>2</sup> AMPHOS 21 Consulting S.L., Passeig de García i Faria, 49-51, 1 – 1 E08019 – Barcelona,  
Spain

<sup>3</sup> Department of Civil and Environmental Engineering, Universitat Politècnica de Catalunya  
- UPC, Jordi Girona 31, 08034 Barcelona, Spain

## ABSTRACT

Estimating the statistical parameters (mean, variance, and integral scale) that define the spatial structure of the transmissivity or hydraulic conductivity fields is a fundamental step for the accurate prediction of subsurface flow and contaminant transport. In practice, the determination of the spatial structure is a challenge because of spatial heterogeneity and data scarcity. In this paper, we describe a novel approach that uses time drawdown data from multiple pumping tests to determine the transmissivity statistical spatial structure. The method builds on the pumping test interpretation procedure of Coptý et al. (2011) (Continuous Derivation method, CD), which uses the time-drawdown data and its time derivative to estimate apparent transmissivity values as a function of radial distance from the pumping well. A Bayesian approach is then used to infer the statistical parameters of the transmissivity field by combining prior information about the parameters and the likelihood function expressed in terms of radially-dependent apparent transmissivities determined from pumping tests. A major advantage of the proposed Bayesian approach is that the likelihood function is readily determined from randomly generated multiple realizations of the transmissivity field, without the need to solve the groundwater flow equation. Applying the method to synthetically-generated pumping test data, we demonstrate that, through a relatively simple procedure, information on the spatial structure of the transmissivity may be inferred from pumping tests data. It is also shown that the prior parameter distribution has a significant influence on the estimation procedure, given the non-uniqueness of the estimation procedure. Results also indicate that the reliability of the estimated transmissivity statistical parameters increases with the number of available pumping tests.

Register for free at <https://www.scipedia.com> to download the version without the watermark

## 1. INTRODUCTION

The modeling of groundwater flow and contaminant transport has evolved in recent decades into a valuable tool for the analysis of subsurface systems. Such modeling efforts require mapping the flow parameters - most notably transmissivity ( $T$ ) or hydraulic conductivity ( $K$ ) - over the domain of interest. Numerous field investigations have however demonstrated that hydrogeological parameters are highly heterogeneous, displaying complex patterns of spatial variability (e.g., *Gelhar* 1993; *Rubin*, 2003, *Sudicky et al.* 2010). Because flow and transport are strongly influenced by the heterogeneity of the subsurface system, incorporating the spatial variability of the underlying parameters is essential for the accurate evaluation of groundwater resources, and in particular for the prediction of contaminant transport as a necessary step for the design and implementation of groundwater remediation activities (e.g., *Sanchez-Vila and Fernandez-Garcia*, 2016).

Complexity in hydrogeological patterns and the lack of detailed data have led researchers to formulate the flow and transport problem within a stochastic framework. With such an approach, flow parameters are defined by spatial random functions whose spatial structure can adequately be expressed in terms of few low-order statistical parameters, namely the spatial mean, variance, and integral scale, which jointly define the covariance function or semi-variogram (*Kitanidis*, 1997; *Renard*, 2007). These statistical parameters are typically

determined from measurements of the attribute of interest, provided that a sufficiently large number of data with adequate spatial coverage is available.

Groundwater flow and solute transport are strongly affected by the spatial distribution of  $T$ . At most sites, the number of  $T$  estimates determined from the interpretation of pumping tests is quite limited, hindering the accurate determination of the  $T$  covariance function. Moreover, traditional pumping test interpretation methods, such as those based on log-log plots (*Theis*, 1935) or semilog plots (*Cooper and Jacob*, 1946), generally yield single estimates of the flow parameters, which hardly provide information about the underlying heterogeneity. In fact, this averaging process results in  $T$  estimates with a smaller variance and a larger integral scale as compared to the actual point distributions, and hence, cannot be used to simulate the impact of small to medium scale variability, which is of interest in many field applications.

These limitations motivated many researchers in the last three decades to examine the impact of spatial heterogeneity on the analysis of pumping tests and investigate whether information about the spatial variability of the flow parameters can be inferred from pumping tests (a

review of methods and solutions was provided by *Sanchez-Vila et al.*, 2006). A very early study is *Barker and Herbert* (1982), who considered the effect of a high hydraulic conductivity anomaly embedded in an otherwise uniform aquifer. *Butler* (1988) used the *Cooper and Jacob* (1946) method to investigate the effect of a  $T$  anomaly on the interpreted transmissivity; it was shown that, for observation wells located at large distances from the pumping well, the perturbed non-uniform aquifer behaves as a homogeneous aquifer. On the other hand, *Butler* (1990) showed that the  $T$  values estimated with the *Theis* (1935) method place more weight on the local  $T$ , defined as the  $T$  in the vicinity of the pumping well. *Feitosa et al.* (1994) developed an inverse procedure for the estimation of the transmissivity as a function of distance from the pumping well for the case when the transmissivity field consists of a series of concentric homogeneous rings.

For spatially variable  $T$  fields (i.e.,  $T$  fields that are not defined in terms of a deterministic perturbation but that are individual realizations of a random field), *Meier et al.* (1998) and *Sanchez-Vila et al.* (1999) showed that the transmissivity obtained with the *Cooper and Jacob* (1946) is close to the spatial geometric mean of the  $T$  field, regardless of the location of the observation point. On the other hand, the estimated storativity ( $S$ ) varies spatially, demonstrating how the interpretation method significantly translates the heterogeneity in transmissivity into spatially variable  $S$  estimates. This finding was further confirmed by

*Trinchero et al.* (2008), who provided an analytical relationship between the estimated storativity and the porosity inferred from tracer test data (the latter parameter was considered as an indicator of transport connectivity).

*Coptý and Findikakis* (2004a) examined the sensitivity of transient drawdown in pumping tests to the statistical parameters describing the spatial structure of  $T$ , and noted that the time derivative of the drawdown is particularly sensitive to the heterogeneity in  $T$ . *Oliver* (1993) and *Knight and Kluitenberg* (2005) used the Frechet kernel to evaluate the sensitivity of the drawdown to the spatial variability of  $T$  and  $S$ . *Leven and Dietrich* (2006) used sensitivity coefficients to assess the influence of the spatial variability of  $T$  and  $S$  on the interpretation of pumping tests, leading to time-dependent interpreted parameters. *Avci et al.* (2011, 2013) developed a numerical method for the estimation of the variability of the  $T$  and  $S$  as a function of pumping time; the method could be used as a diagnostic tool to identify some aquifer system characteristics. *Avci et al.* (2014) evaluated the performance of a number of analytical methods for the estimation of the variation of the transmissivity with radial distance. Recently, *Pechstein et al.* (2016) discussed the relationship of the interpreted  $T$

values derived from pumping tests to the underlying spatial variability of the  $T$  field. The authors showed numerically that the interpreted  $T$  value that best reproduces the pumping test data in confined heterogeneous aquifers is a weighted average of the point  $T$  values which uses the temporal derivative of the Frechet kernel as a spatial weight.

*Copty et al.* (2008) and *Trinchero et al.* (2008a) considered the influence of spatial variability of the transmissivity on pumping tests conducted in leaky aquifers. A significant difference between flow towards a well in a confined non-leaky versus a leaky aquifer is that in the former case the cone of depression continues to expand with time, while in the latter a steady state condition is reached. As a result, the response of a pumping test in a leaky aquifer is more sensitive to variations in the local transmissivity in the vicinity of the well, as compared to the case of a confined aquifer.

A number of studies have attempted to estimate directly, from pumping test data, the statistical spatial structure of the transmissivity field, commonly expressed in terms of two statistical parameters: variance and integral scale. *Copty and Findikakis* (2004b) examined the relation of the time-derivative of the drawdown to the integral scale and the variance of the log-transmissivity field. *Neuman et al.* (2004, 2007) developed a graphical approach that uses steady-state drawdown data for the estimation of the  $T$  variance and integral scale. *Riva et al.* (2009) applied this type-curve method to field data from the site of Poitiers, France.

*Firmiani et al.* (2006) used an expression of the equivalent hydraulic conductivity for steady-state radially convergent flow towards a well in a heterogeneous aquifer to estimate the variance and integral scale of  $K$ . *Zech et al.* (2012) developed an analytical expression for the steady state drawdown due to pumping in a heterogeneous aquifer using the Coarse Graining upscaling method (*Attinger*, 2003), a method subsequently applied to real pumping test data from the Horkheimer Insel test site in Germany (*Zech et al.*, 2015). This latter paper also discusses the quantity and spatial coverage of the data needed to obtain reliable estimates of the statistical parameters of the transmissivity field. *Zech et al.* (2016) extended the analysis to transient flow and showed that the number of measurements needed to obtain reliable estimates of the transmissivity spatial structure is reduced compared to steady state pumping tests.

In parallel efforts, and to overcome the scarcity of hydrological data commonly encountered in field applications, a number of researchers have proposed incorporating additional secondary data in the identification of subsurface parameters such as geophysical data (see recent reviews such as *Binley et al.*, 2015; *Slater*, 2007; *Rubin and Hubbard*, 2005). Novel

field data acquisition techniques, such as hydraulic tomography (e.g., *Butler et al.*, 1999; *Yeh, and Liu*, 2000; *Zhu and Yeh*, 2005; *Yin and Illman*, 2009; *Illman et al.*, 2015) and direct push technologies (*Butler et al.*, 2007; *Dietrich et al.*, 2008; *Bohling et al.*, 2012) have also been proposed. These approaches have been shown to have several benefits; most notably they allow for the collection of dense hydraulic head data in response to groundwater pumping that allows for the estimation of the three-dimensional hydraulic conductivity distribution in the vicinity of the tests. Despite these advantages, their application to routine field problems remains limited due to the relatively large costs associated and the difficulty of solving the groundwater inverse problem.

Despite these recent developments, the determination of the underlying statistical spatial structure of the transmissivity field from pumping test data remains a challenge. In a recent study, *Coptý et al.* (2011) developed an interpretation method for pumping tests, denoted as the Continuous Derivation (CD) method. The CD method uses the transient drawdown data and its time derivative to estimate interpreted transmissivities as a function of the radial distance,  $T_i(r)$ . It was shown by *Coptý et al.* (2011) that  $T_i(r)$  is close to the geometric mean of the  $T$  values over a radially increasing volume,  $T_g(r)$ . The function  $T_g(r)$  varies from the transmissivity at the well for small values of  $r$ , to the geometric mean of the entire field, for

large  $r$  values. In the current study, we extend the work of *Coptý et al.* (2011) by examining whether  $T_i(r)$  can be used to infer the spatial structure of the transmissivity field. The goal is

thus to develop a relatively simple pumping test interpretation method that can help in the definition of relevant characteristics of the local scale transmissivity spatial structure without the need for complex inverse modeling. We primarily focus on time-drawdown data derived from pumping tests, which remains a widely used technique for subsurface parameter estimation.

For the sake of completion, we present in Section 2 the main features of the CD method, followed by the presentation of the Bayesian approach used to infer the spatial structure of the transmissivity field, namely the variance and the integral scale. Section 3 describes a numerical application of the proposed Bayesian method and discusses its potential applications and limitations.

## 2. Pumping Test Interpretation Method

### 2.1. The Continuous Derivation Method (CD)

For pumping tests conducted in heterogeneous aquifers, the cone of depression due to pumping expands in time. At early times the apparent transmissivity is close to the  $T$  value in the immediate vicinity of the well (order of few meters), while at later times it is some weighted average of the transmissivity of a much larger region around the well. The term “apparent” is used here in accordance with the terminology of *Sanchez-Vila et al.*, 2006 which refers to an estimate of the parameter that is function of space and that satisfies some relationship such as the Theis solution (*Theis*, 1935). The CD method (*Coptly et al.*, 2011) captures the full temporal transition between the local  $T$  value and the estimate obtained using late time data. The estimation method relies on the time-derivative of the drawdown because this is more sensitive than the drawdown itself to spatial variation of transmissivity (e.g., *Bourdet*, 2002).

For two-dimensional flow towards a well in a confined aquifer, the time-dependent drawdown is given by the classical Theis’ solution:  $s(t, r) = \frac{Q}{4\pi T} W(u)$ , where  $u = \frac{r^2 S}{4tT}$ ,  $W(u)$  is the well (i.e., the exponential integral) function,  $Q$  is the pumping rate,  $r$  is the separation distance between the pumping and observation wells,  $t$  is time, and  $S$  is storativity. The ratio of the drawdown to the drawdown time derivative,  $s'(t, r)$ , can be written as (*Coptly et al.*, 2011):

$$\gamma_c = \frac{s}{s'} = \frac{2.35}{W(u) \exp(u)} \quad (1)$$

A plot of the function  $\gamma_c$  is shown in Figure 1. It is observed that  $\gamma_c$  increases monotonically with dimensionless  $1/u$  (equivalent to a dimensionless time). For a given pumping test, the ratio of the observed drawdown at any time  $t$  to its time derivative provides an estimate of  $u$  from (1). From the estimated  $u$  value, the interpreted transmissivity and storativity ( $T_i$  and  $S_i$ , respectively) corresponding to that particular moment in time are then estimated as:

$$T_i(t) = \frac{Q}{4ps(t)} W(u); \quad S_i(t) = \frac{4tT_i u}{r^2} \quad (2)$$

Applying the above procedure repetitively to the full duration of the test yields time-dependent estimates of the flow parameters. Thus, the CD method provides estimates of the flow parameters that change with time, in contrast to conventional methods (e.g., the Theis method) that lump all observed drawdown together to estimate single representative values of  $T$  and  $S$ .



197

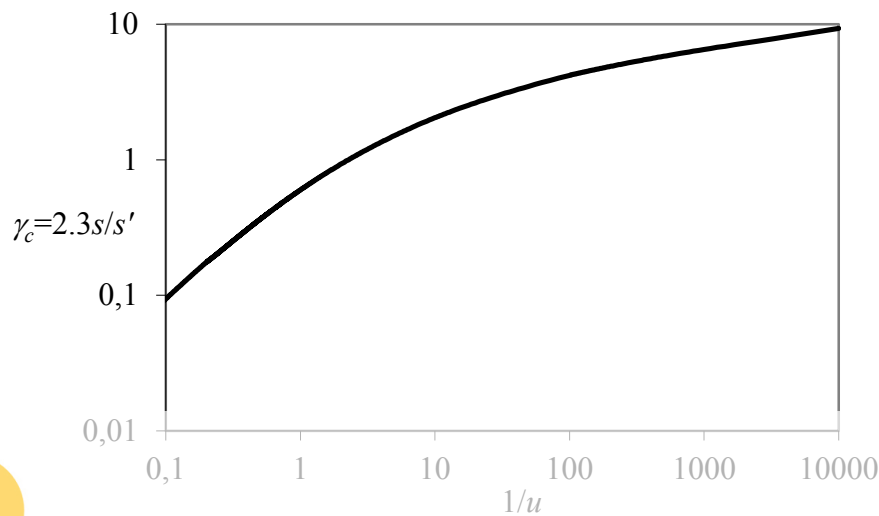


Figure 1. Plot of  $\gamma_c$  as a function of  $1/u$  (modified from *Copty et al.*, 2011)

198

199

200

201

202

203

204

Through sensitivity analysis of the drawdown and its derivative to variations in the transmissivity, the interpreted transmissivity  $T_i$ - $t$  relationship is mapped into a  $T_i$ - $r^*$  relationship, where  $r^*$  is a radial distance computed as (*Copty et al.*, 2011):

$$r^* = \sqrt{\frac{4tT}{1.65S}} \quad (3)$$

Register for free at <https://www.scipedia.com> to download the version without the watermark

205

206

207

208

209

210

211

212

213

214

215

## 2.2. Bayesian Approach for the Estimation of the Variance and Integral Scale

216

217

218

219

Since the estimation of the transmissivity variance and integral scale is generally difficult and therefore associated with a high level of uncertainty, we define these two parameters as random functions. Denoting  $V$  and  $I$  as the variance and integral scale random functions, respectively, the primary goal of this paper is to estimate their conditional joint probability



density function (pdf),  $f_{V,I}^c(v,i|Y_1 \cdots Y_N)$ , where  $Y_1 \cdots Y_N$  denotes the drawdown data from  $N$  available pumping tests. The superscript  $c$  denotes conditional.

Using the CD method, the drawdown data from each pumping test is converted to the geometric mean of the transmissivity as a function of radial distance from the well,  $T_g(r)$ . Interpretation of each pumping test is done separately. If data from more than one observation well are present for the same pumping test, they would yield similar  $T$  estimates as they would be sampling the same aquifer volume. Under such conditions, it is sufficient to use data from only one observation well. This redundancy in information has also been noted by other researchers, such as *Leven and Dietrich* (2006) and *Bohling and Butler* (2010), who demonstrated the issue of reciprocity of sequential pumping tests when pumping and monitoring wells are reversed. Limitations of reciprocity have been also explored elsewhere (e.g., *Delay et al.*, 2012; *Sanchez-Vila et al.*, 2016). Substituting each pumping test by the transmissivity functions derived from the available pumping tests, the conditional joint pdf is rewritten as  $f_{V,I}^c(v,i|T_{g,1}(r) \cdots T_{g,N}(r))$ , where  $T_{g,1}(r) \cdots T_{g,N}(r)$  denotes the transmissivity estimates derived from pumping tests 1, ...,  $N$ . In other words, the goal here can be restated as the estimation of the joint pdf of  $V$  and  $I$  conditioned on the estimates of the geometric mean of the  $T$  field as a function of radial distance derived from all available pumping tests. To simplify the notation, the variable  $r$  is dropped from the ensuing derivations. It is however important to note that  $T_{g,k}$  is not a single value but rather a full function of  $r$ .

Using Bayes' Theorem on conditional probability (e.g. *Tarantola*, 1987), the joint pdfs are:

$$f_{V,I}^c(v,i|Y_1 \cdots Y_N) = f_{V,I}^c(v,i|T_{g,1} \cdots T_{g,N}) = \frac{f_T(T_{g,1} \cdots T_{g,N}|v,i) \times f_{V,I}(v,i)}{f_T(T_{g,1} \cdots T_{g,N})} \quad (4)$$

where

$f_T(T_{g,1} \cdots T_{g,N}|v,i)$  is the likelihood of observing  $T_{g,k}$  given that variance and integral scale values are  $v$  and  $i$ , respectively. This pdf can be seen as the reverse of the desired pdf,  $f_{V,I}^c(v,i|T_{g,1} \cdots T_{g,N})$

$f_T(T_{g,1} \cdots T_{g,N})$  is the unconditional pdf of observing  $T_{g,1} \cdots T_{g,N}$

247  $f_{V,I}(v,i)$  is the prior joint pdf of observing the variance and integral scale values  
 248  $v$  and  $i$ , respectively.

249 The pdf in the denominator of (4) is denoted as  $\omega$ , and can be expressed from the definitions  
 250 of the marginal and conditional probabilities (Tarantola, 1987) as:

$$251 \quad \omega = f_T(T_{g,1} \cdots T_{g,N}) = \int_{V,I} f_T(T_{g,1} \cdots T_{g,N} | v, i) \times f_{V,I}(v, i) dv di \quad (5)$$

252 In words, the pdf of  $T_{g,1} \cdots T_{g,N}$  is equal to the probability of observing  $T_{g,1} \cdots T_{g,N}$  given that  
 253  $V=v$  and  $I=i$ , integrated over all possible values of  $V$  and  $I$ ;  $\omega$  is a normalizing parameter that  
 254 guarantees that (4) is a proper pdf; that is:  $\int_{V,I} f_{V,I}^c(v, i | T_{g,1} \cdots T_{g,N}) dv di = 1$

255 If the separation distances between the different pumping tests is large such that the cones  
 256 of depression do not significantly overlap (consequently, there is little redundancy in the  
 257 data), then the pumping tests can be treated as independent (i.e., they sample different  
 258 volumes of the aquifer). The likelihood function  $f_T(T_{g,1} \cdots T_{g,N} | v, i)$  can be re-written as a  
 259 product of the individual pdfs:

$$260 \quad f_{V,I}^c(v, i | Y_1 \cdots Y_N) = \frac{1}{\omega} f_T(T_{g,1} | v, i) \cdots f_T(T_{g,N} | v, i) f_{V,I}(v, i) \quad (6)$$

261 where

$$262 \quad \omega = \int_{V,I} f_T(T_{g,1} | v, i) \cdots f_T(T_{g,N} | v, i) f_{V,I}(v, i) dv di \quad (7)$$

263 Equation (6) states that the pdf of  $V$  and  $I$  conditional on the available pumping test data can  
 264 be expressed in terms of products of  $N+1$  pdfs. The first one,  $f_{V,I}(v, i)$ , is the prior joint pdf  
 265 of  $V$  and  $I$ , which reflects the level of knowledge of the site *prior* to conducting the pumping  
 266 tests. Such information can be derived from previously conducted geologic or geophysical  
 267 studies, or adopted from other sites with similar characteristics. In the absence of  
 268 information,  $f_{V,I}(v, i)$ , can be taken as some uniform (uninformative) distribution that  
 269 includes all possible values, reflecting the lack of knowledge of the site.

270 The remaining  $N$  pdfs are  $f_T(T_{g,k} | v, i)$   $k = 1, \cdots N$ ; i.e., the individual likelihood functions of  
 271 observing  $T_{g,k}$  given that the aquifer variance and integral scale are  $v$  and  $i$ , respectively, in  
 272 pumping test  $k$ . As it will be described in the following subsection, the likelihood functions  
 273 can be readily computed without the need for any inverse modeling by generating multiple  
 274 realizations of the transmissivity field with different values of  $V$  and  $I$ , computing the

resultant pdf of the geometric mean of the generated transmissivity fields and then evaluating the likelihood of  $T_{g,k}$ . Hence, it can be seen that the desired pdf,  $f_{V,I}^c(v,i|Y_1 \cdots Y_N)$  depends on both prior information about the site,  $f_{V,I}(v,i)$ , and the information derived from the pumping test,  $f_T(T_{g,k}|v,i) k=1, \cdots N$ .

279

Finally, the marginal pdfs of  $V$  and  $I$  are computed as:

$$f_V^c(v|Y_1 \cdots Y_N) = \int_I f_{V,I}^c(v,i|Y_1 \cdots Y_N) di, \quad (8)$$

$$f_I^c(i|Y_1 \cdots Y_N) = \int_V f_{V,I}^c(v,i|Y_1 \cdots Y_N) dv. \quad (9)$$

The expected values of the variance and integral scale can be computed from the integral of the conditional joint pdf of  $V$  and  $I$ ,  $f_{V,I}^c(v,i|Y_1 \cdots Y_N)$ :

$$E[I] = \int_{V,I} i f_{V,I}^c(v,i|Y_1 \cdots Y_N) dv di, \quad (10)$$

$$E[V] = \int_{V,I} v f_{V,I}^c(v,i|Y_1 \cdots Y_N) dv di. \quad (11)$$

287

### 2.3. Estimation of the likelihood function $f_T(T_{g,1} \cdots T_{g,N}|v,i)$

This section describes the method used to estimate the likelihood function  $f_T(T_{g,1} \cdots T_{g,N}|v,i)$ . It is assumed that  $\ln T$  is a multivariate Gaussian random spatial function with exponential semi-variogram. Other semi-variogram functions could also be considered. Multiple realizations ( $n=1000$ ) of the natural logarithm of the transmissivity were randomly generated for various  $V$  and  $I$  values using the Turning band method (*Mantoglou and Wilson, 1982*). The geometric mean of the transmissivity over a circular area with radius  $r$  located at the center of the generated domain was computed as:

$$T_g(r) = \exp \left[ \int_{r=0}^r \ln(T) dA \right] \quad (12)$$

Figure 2 displays  $T_g(r)$  for randomly selected transmissivity fields with variance  $V=1$ . The radial distance in the figure is normalized by the integral scale,  $I$ , while the ensemble geometric mean,  $T_{g,o} = T_g(r \rightarrow \infty)$  was used to normalize the vertical axis. It can be seen

that the variability of  $T_g(r)$  decreases as  $r$  increases. For radial distances larger than about  $20I$ ,  $T_g(r)$  approached the ensemble geometric mean for all of the generated transmissivity fields.

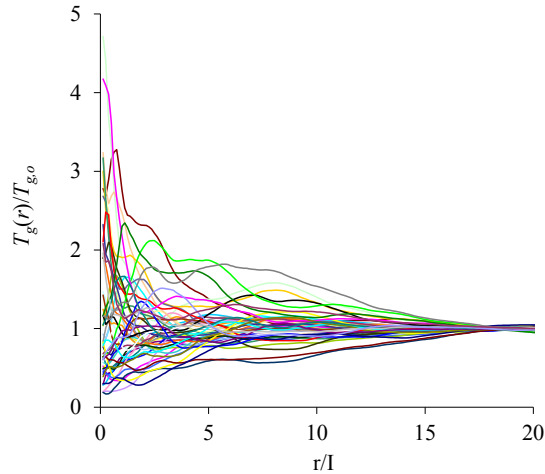
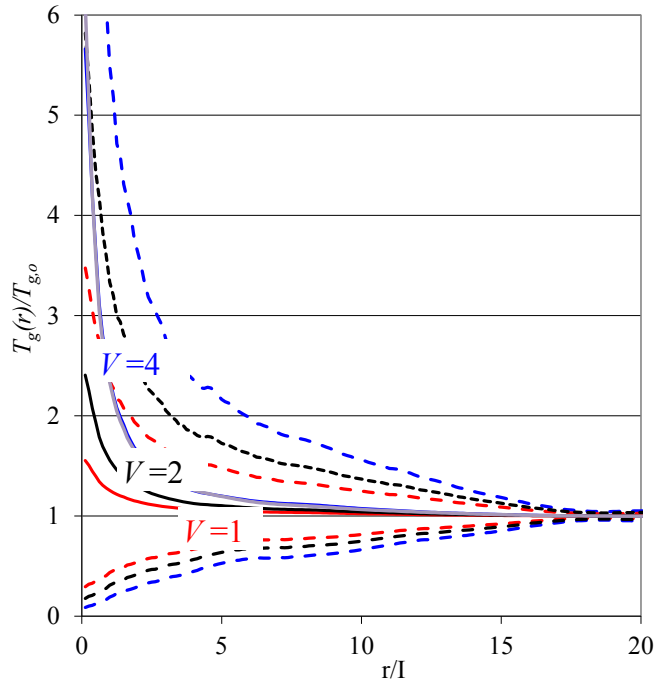


Figure 2.  $T_g(r)$  as a function of radial distance for randomly selected transmissivity fields with  $V=1$ .  $T_g(r)$  is normalized by the ensemble mean of  $T$  used in data generation. The distance  $r$  is normalized by the integral scale,  $I$ .

Figure 3 shows the expected value and upper/lower deciles of  $T_g(r)$  for  $V=1, 2$  and  $4$ . The expected value was computed for each distance  $r$  as the arithmetic average of the 1000 realizations. Similar curves for other values of the variance could be developed readily. Analysis of the generated realizations shows that 1000 simulations were sufficient (with error less than 1%). Figure 3 shows that for  $r=0$  the expected value is simply the arithmetic mean of the transmissivity at the well. For  $r/I > 20$ ,  $T_g(r)$  of each realization approaches the ensemble geometric mean and hence, the expected value over all realizations would also approach the ensemble geometric mean. The semi-variogram model selected influences the rate of change with distance, but not the end points.

Although Figure 3 depicts only the average and upper/lower deciles, it is evident that for a particular value of  $V$  and  $r/I$ , there is a range of possible values of  $T_g(r)$ . This range increases with the increase in the variance value, and decreases as  $r/I$  increases. This figure also shows overlap among the different set of curves; e.g., for a given distance, the possible range of values of  $T_g$  obtained with variance  $V=2$  is fully comprised within the range spanned by  $V=4$ .

323 This overlap has an influence on the Bayesian estimation, as discussed in detail in section  
 324 3.2.



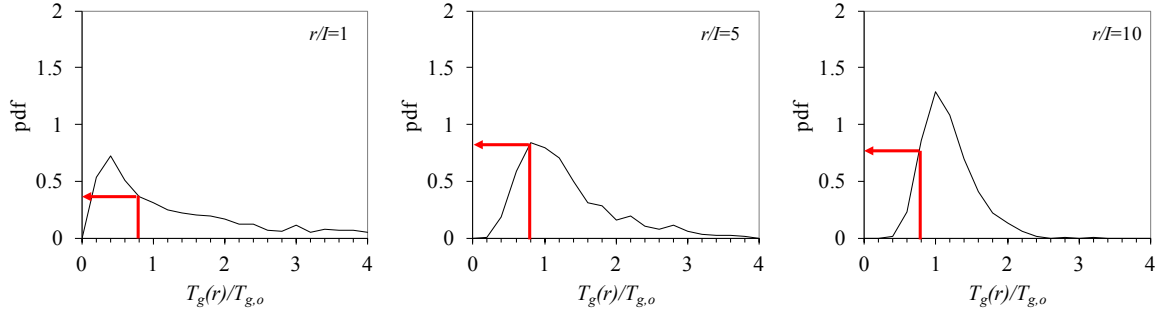
325  
 326 Figure 3. Expected value (solid line) and upper/lower deciles (dashed lines) for  $V=1, 2$  and  
 327 4. The red, black and blue lines correspond to  $V=1, 2$ , and 4, respectively.  $T_g(r)$  is normalized  
 328 by the geometric mean of the transmissivity,  $T_{go}$  used in data generation.

329  
 330 Based on the information shown in Figure 3, it is possible to construct a distribution of all  
 331 possible  $T_g(r)$  values corresponding for each  $V$  and  $r/I$  pairs. Figure 4 shows the pdfs of  $T_g(r)$   
 332 at 3 different distances:  $r/I=1, 5$  and 10, and for  $V=1$ . As distance increases, the statistical  
 333 distribution becomes narrower and less skewed. It is important to note that these pdf's are  
 334 computed only once and can be used in other problems provided the semi-variogram model  
 335 is kept.

336 Figure 4 also shows a sample calculation of the likelihood function for a  $T_g(r)$  obtained from  
 337 a given pumping test. Starting from the  $T_g(r)$  values derived from the pumping test, one can  
 338 calculate the pdf corresponding for each  $V$  and  $I$  pairs. Because the pdf's depicted in Figure  
 339 4 are for particular values of  $V$  and  $I$ , this calculation has to be repeated for all possible  $V$   
 340 and  $I$  pairs as defined by their prior joint distribution,  $f_{V,I}(v, i)$ .

341 According to the Bayesian formulation (Equation 4), the desired joint conditional pdf of  $V$   
 342 and  $I$  is function of the product of the likelihood function and the prior distribution. If for a

343 given pair  $(v, i)$ , the product of  $f_{V,I}(v, i)$ , and  $f_T(T_{g,1} \cdots T_{g,N} | v, i)$  is small, the probability of  
 344 the transmissivity field having these  $v$  and  $i$  values would also be small. On the other hand,  
 345 if this product is large, this would mean that this  $(v, i)$  pair is more likely.  
 346



347  
 348 Figure 4: pdfs of  $T_g(r)$  at  $r/I=1, 5$  and  $10$  and for  $V=1$ . The red arrow represents the likelihood  
 349 function for an example  $T$  value derived from a particular pumping test  
 350

351 The above discussion illustrates the benefits of formulating the parameter estimation within  
 352 a Bayesian framework. First, it incorporates the information inferred from the pumping test  
 353 data, as well as any prior information about the site. Second, the Bayesian formulation  
 354 simplifies the calculation by expressing the desired conditional pdf,  $f_{V,I}^c(v, i | T_{g,1} \cdots T_{g,N})$  in  
 355 terms of its reciprocal,  $f_T(T_{g,1} \cdots T_{g,N} | v, i)$  (Eq. 4). Whereas the former can be viewed as a form  
 356 of the inverse problem and its evaluation is not straight forward,  $f_T(T_{g,1} \cdots T_{g,N} | v, i)$  can be  
 357 readily determined from the randomly generated transmissivity fields corresponding to the  
 358  $v$  and  $i$  values as presented above without the need for any inverse modeling. Third, the  
 359 Bayesian approach provides an estimate of the entire pdf based on prior information and the  
 360 pumping test data and, as such, provides a measure of the uncertainty of the estimates.

361 In summary, we list below the main steps for the estimation of the conditional joint pdf of  $V$   
 362 and  $I$ ,  $f_{V,I}^c(v, i | T_{g,1} \cdots T_{g,N})$ :

- 363 1. Given  $N$  pumping tests, the geometric transmissivity as a function of radial distance  
 364  $T_{g,1}(r) \cdots T_{g,N}(r)$  is estimated using the CD method. Each pumping test is analyzed  
 365 separately.
- 366 2. The prior joint pdf of  $V$  and  $I$ ,  $f_{V,I}(v, i)$ , is defined based on prior information about the  
 367 site.

- 368 3. For the available pumping tests, the likelihood function  $f_T(T_{g,1} \cdots T_{g,N} | v, i)$  is determined  
 369 from Figures 3 and 4. By assuming the pumping tests are sufficiently far and, therefore,  
 370 can be treated as independent, the likelihood function is expressed as a product of the  
 371 likelihood functions of the individual pumping tests (Eq. 6). It is important to note that  
 372 these figures do not require the simulation of the groundwater flow equation; they were  
 373 developed by generated multiple realizations of the transmissivity field and averaging  
 374 the  $T$  as a function of radial distance. The calculation of the likelihood function is  
 375 repeated for all possible  $v$  and  $i$  pairs as defined by their prior distribution (step 2).  
 376 4. The normalizing parameter,  $\omega$ , is calculated from Eq. (5) or Eq. (7) if the pumping tests  
 377 treated as independent.  
 378 5. The desired conditional pdf is finally computed according to Eq. (4) or Eq. (6). The  
 379 marginal distributions of  $V$  and  $I$  are determined from Eq (8) and Eq. (9), respectively.  
 380

### 381 3. Application

#### 382 3.1. Data Generation

383 To demonstrate the above parameter estimation procedure, the procedure was tested using  
 384 1000 synthetic pumping tests conducted in confined heterogeneous aquifers. The  
 385 heterogeneous transmissivity fields were generated using the turning bands method. It was  
 386 assumed that the natural log transform of the transmissivity is a multivariate Gaussian  
 387 random spatial function with zero mean ( $T_g=1$ ), an exponential semi-variogram, with  
 388 variance,  $V=1$ , and integral scale,  $I= 8$  length units (lu). Storativity was assumed to be  
 389 uniform, as field data usually indicate that the spatial variation in storativity is less than that  
 390 of the transmissivity. The storativity value used in all simulations was 0.0001; which is a  
 391 typical value for a confined aquifers (*Domenico and Schwartz, 1997*).

392 The flow domain was assumed to be 481 by 481 lu. A fully penetrating pumping well was  
 393 placed at the center of the domain. The observation point was assumed to be at a distance of  
 394  $I/8$  from the pumping well. Constant head conditions were prescribed along the outer  
 395 boundaries of the domain. The duration of the pumping test was  $\tau=1$ , while the pumping rate  
 396 was fixed at  $Q=2$  (using consistent units for both  $\tau$  and  $Q$ ). Pumping tests were terminated  
 397 before the drawdown data were affected by boundary effects.



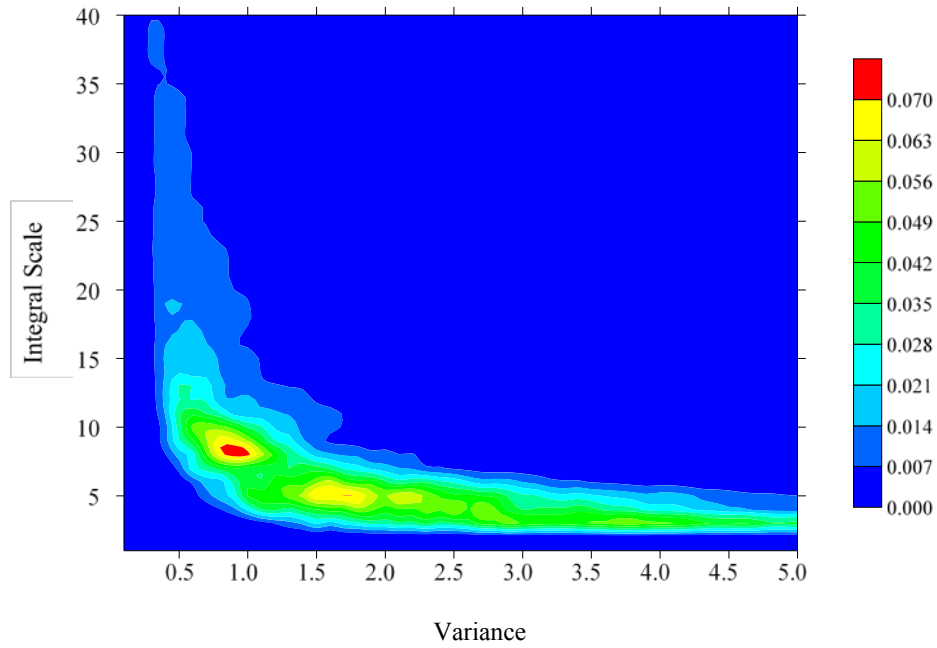
398 The pumping tests were simulated using MODFLOW (Harbaugh *et al.*, 2000). A uniform  
 399 grid of 1 by 1 lu was used. The drawdown data were analyzed using the CD method yielding  
 400 one  $T_g(r)$  for each of the 1000 simulated pumping tests. Using the proposed Bayesian  
 401 approach, the inferred  $T_g(r)$  was then used to estimate the variance and integral scale. To  
 402 assess the robustness of the proposed method, a Monte Carlo approach was adopted. First,  
 403 each of the  $T_g(r)$  curves were used independently to estimate the variance and integral scale  
 404 of the  $T$  field. This corresponds to the case when only a single pumping test is present ( $N=1$ ).  
 405 The method was then repeated by combining 5 and 10 pumping tests ( $N=5$  and  $N=10$ ,  
 406 respectively) to test the performance of the method when multiple wells are present.  
 407 The Bayesian estimation requires the definition of a prior distribution for the parameters of  
 408 interest (variance and integral scale). In the present analysis, the prior distribution of the  
 409 variance was assumed to be uniform between 0 and 5,  $U_V(0,5)$ . This range encompasses  
 410 typical variance values encountered in the field (Gelhar, 1993). The prior pdf of the integral  
 411 scale was also assumed to be uniform between 0 and 40 lu,  $U_I(0,40)$ . The uniform  
 412 distributions are the least informative distributions in terms of priors, requiring only the  
 413 definition of upper limits (5 and 40 lu, respectively). The corresponding joint prior pdf is  
 414  $f_{V,I}(v,i)=1/5 \times 1/40=0.005$ . The joint pdf is also uniformly distributed which means that all  $v$   
 415 and  $i$  pairs falling between the lower and upper limits of  $V$  and  $I$  respectively have the same  
 416 probability of occurring. To assess the sensitivity of the prior distribution on the estimation  
 417 of the variance and integral scale, the analysis was also repeated assuming the prior  
 418 distributions of the variance and the integral scale are  $U_V(0,3)$  and  $U_I(0,30)$ , respectively,  
 419 which are closer to the parameter values used in data generation.

420

### 421 3.2. Results

422 The parameter estimation procedure was repetitively applied to all 1000 pumping tests.  
 423 Figure 5 shows a randomly selected example of the conditional joint pdf of the variance and  
 424 integral scale obtained with the Bayesian estimation procedure. The true variance and  
 425 integral scale used in the data generation are 1 and 8 lu, respectively. The number of available  
 426 pumping tests was 5. The conditional pdf joint should be contrasted to the prior  
 427  $f_{V,I}(v,i)=0.005$ . This figure shows that conditioning on the pumping test data shifts the pdf  
 428 from the diffuse prior towards the true values of the variance and integral scale ( $v=1$ ,  $i=8$  lu).  
 429 The range of the more likely values of the variance and integral scale significantly decreased.

430



431

432 Figure 5. Example of the conditional joint pdf of the variance and integral scale based on  
 433 data from 5 pumping tests. The prior distributions of the variance and integral scale are  
 434  $U_V(0,5)$  and  $U_I(0,40)$  which correspond to a prior pdf  $f_{V,I}(v,i)=0.005$ . The true values are  
 435  $V=1$  and  $I=8$  lu.

436

437 The marginal distributions of the integral scale and variance for 3 randomly selected cases  
 438 are shown in Figure 6. Each of these conditional pdfs were computed assuming 5 pumping  
 439 tests were available. The mean of the marginal pdfs of the integral scale for the three  
 440 randomly selected cases were 5.8, 9.2 and 17 lu. The mean of the marginal pdfs of the  
 441 variance on the other hand were 2.4, 1.8 and 0.86. For comparison, the prior pdfs of  $V$  and  $I$   
 442 are also shown in this figure. The corresponding means of the prior pdfs of the integral scale  
 443 and variance were 20 lu and 2.5, respectively. These results show that the conditional  
 444 variance and integral scale marginal pdfs are closer to the true values ( $V=1$ ,  $I=8$  lu) compared  
 445 to the initial prior distribution. The conditional marginal pdfs do exhibit a tail that results  
 446 from the diffuse prior distribution of  $V$  and  $I$ , and the overlap of the likelihood functions  
 447 (Figures 3 and 4).

448

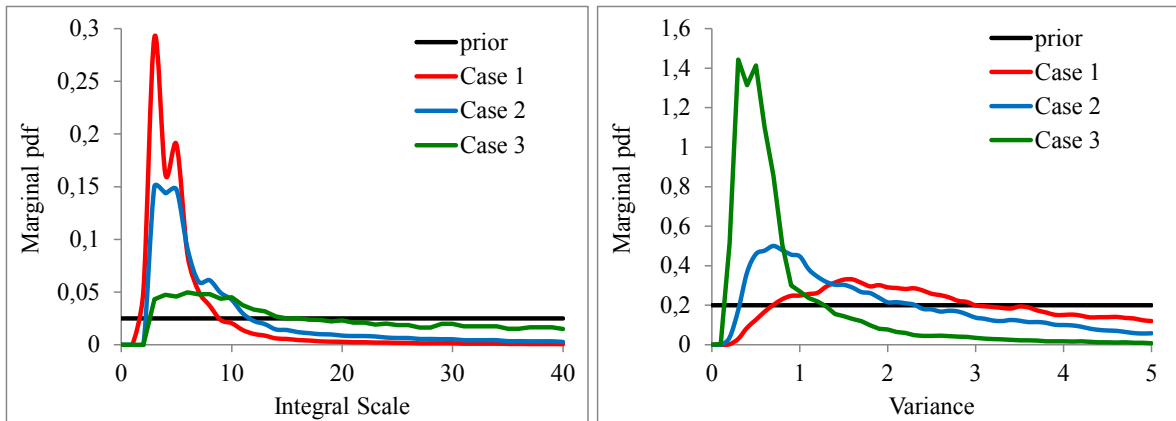


Figure 6. Integral scale and variance marginal pdfs for three randomly selected cases. Each of these cases assumes 5 pumping tests are available. The prior distributions of the variance and integral scale are  $U_V(0,5)$  and  $U_I(0,40)$ . The true values are  $V=1$  and  $I=8$  lu.

Figure 7 presents the histogram of the conditional expected values of the integral scale ( $E[I]$ ) and variance ( $E[V]$ ), from the 1000 Monte Carlo results. The results are computed using 1, 5 or 10 pumping tests. The average of  $E[V]$  and  $E[I]$  over all realization for  $N=1, 5$ , and 10 are shown in Table 1, For comparison, the “true” values of  $V$  and  $I$  used in the generation of the  $T$  fields and the expected values of the prior distribution are also included. Figure 7 and Table 1 demonstrate that the Bayesian updating can be viewed as a weighted average of the prior pdf and the results of the pumping test. Conditioning improves the estimation of the considered variables although, because of the overlap of the different likelihood functions (Figures 3), the resulting histograms still show some spread. Provided there is no redundancy in the data, increasing the number of pumping tests causes the estimates of the variance and integral scale to shift towards the true values.

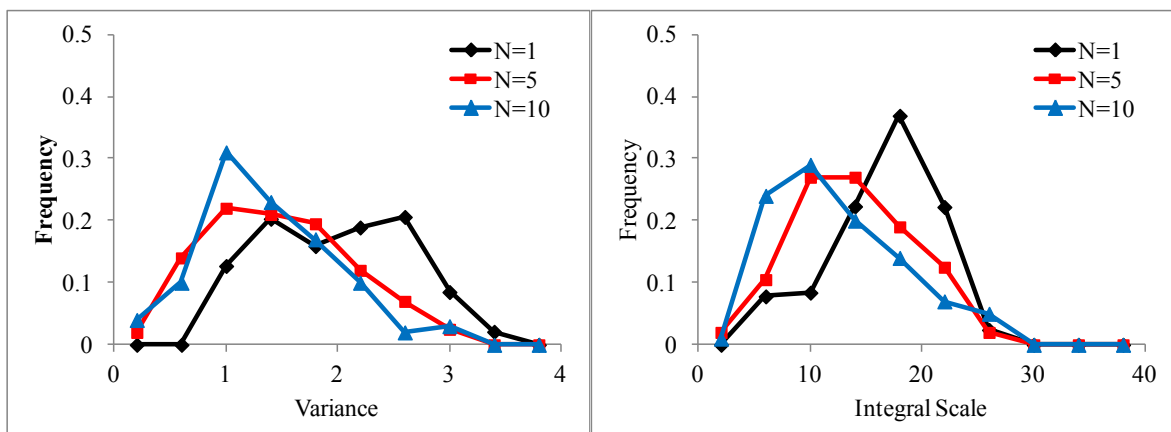


Figure 7. Histograms of  $E[V]$  and  $E[I]$  based on the Monte Carlo analysis, assuming 1, 5 or 10 pumping tests are available. The prior distributions are  $U_V(0,5)$  and  $U_I(0,40)$ , implying expected values of 2.5 and 20 lu, respectively. The true values are  $V=1$  and  $I=8$  lu.

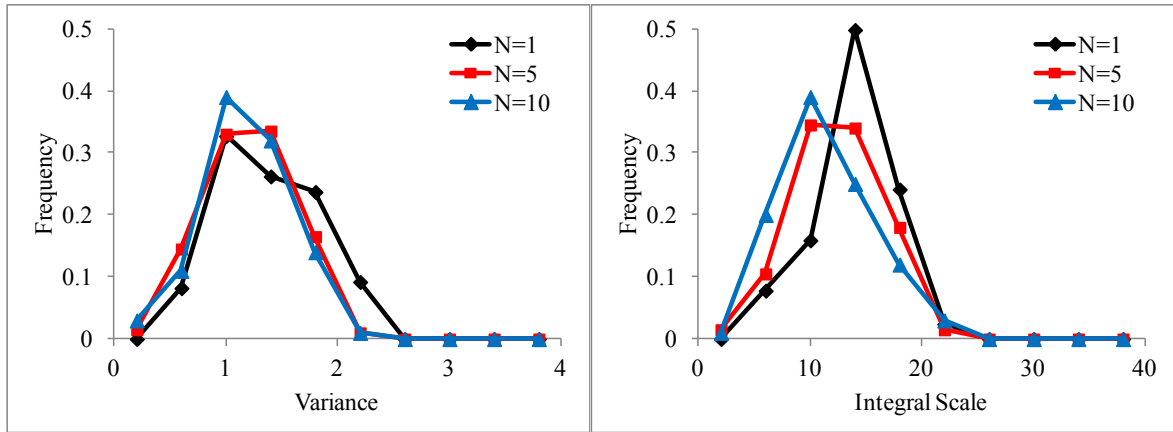
Table 1: Average of  $E[V]$  and  $E[I]$  for all simulations, assuming  $N=1, 5$  or 10 pumping tests are available and for different prior distributions of the variance and integral scale. For comparison, the true values used in the generation of the transmissivity field are also shown

Prior distributions	Number of Pumping Tests	Average of $E[V]$	Average of $E[I]$ , lu
$V$ : Uniform between 0 and 5 $I$ : Uniform between 0 and 40 lu	0	2.5	20
	1	1.96	16.7
	5	1.47	13.9
	10	1.36	12.4
$V$ : Uniform between 0 and 3 $I$ : Uniform between 0 and 30 lu	0	1.5	15
	1	1.36	13.8
	5	1.21	12.5
	10	1.17	11.5
"True" Values of $I$ and $V$		1	8

Note: The average values corresponding to  $N=0$  are the values of the prior distributions before conditioning on the pumping well data

To assess the impact of the prior  $V$  and  $I$  distributions, the parameter estimation procedure was repeated with the same pumping tests, but now assuming that the initial distributions of the variance and integral scales are uniformly distributed between 0 and 3 and between 0 and 30 lu, respectively. Figure 8 shows the histograms of the  $E[V]$  and  $E[I]$  for different number of pumping tests. The corresponding average of  $E[V]$  and  $E[I]$  for all simulations are given in Table 1. With increase in the number of pumping tests,  $E[V]$  and  $E[I]$  move from the expected values of the prior distributions,  $E^p[V] = 1.5$  and  $E^p[I] = 15$  lu, towards the true parameter values,  $V=1$  and  $I=8$  lu. Compared to Figure 7, the impact of the number of tests on the estimation is less significant (in particular for  $E[V]$ ), because the prior estimates were

486 closer to the true values. This demonstrates the benefits of using accurate prior distributions  
 487 in Bayesian estimation procedures provided such information is available.  
 488



489  
 490 Figure 8. Histograms of  $E[V]$  and  $E[I]$ , assuming 1, 5 or 10 pumping tests are available.  
 491 The prior distributions are  $U_V(0,3)$  and  $U_I(0,30)$ , implying expected values of 1.5 and 15 lu,  
 492 respectively. The true values are  $V=1$  and  $I=8$  lu.  
 493

#### 494 4. Summary and Conclusions

495 Modeling of the spatial variability of transmissivity is essential for the accurate simulation  
 496 of groundwater flow and contaminant transport. The spatial variability of  $T$  is commonly  
 497 defined in terms of a semi-variogram or covariance function that is expressed in terms of  
 498 two statistical parameters: the variance,  $V$ , and integral scale,  $I$ . It is therefore important to  
 499 develop simple techniques for the estimation of these two statistical parameters. Despite the  
 500 development in recent years of novel data acquisition techniques, the analysis of drawdown  
 501 data from pumping tests remain the most commonly used technique for the identification of  
 502 subsurface flow parameters. Traditionally, the interpretation of pumping tests generally yield  
 503 single representative (apparent) estimates of the flow parameters. Here we explore whether  
 504 pumping test data can be used to infer the variance and integral scale of the transmissivity,  
 505 two statistical parameters that describe the spatial variability of the underlying transmissivity  
 506 field. Estimates of the variance and integral scale can be employed in the analysis of flow  
 507 and contaminant transport problems and their associated uncertainty, either directly using  
 508 various analytical expressions found in the literature that relate flow and transport attributes

509 to the underlying aquifer heterogeneity, or numerically through the generation of multiple  
 510 realizations of the transmissivity field.

511 The starting point of the present study is the Continuous Derivation method (*Coptý et al.*,  
 512 2011), which uses the drawdown and its time derivative to estimate a function that was  
 513 shown to be close to the geometric mean of the transmissivity field defined over an  
 514 increasing radial distance from the pumping well,  $T_g(r)$ . Analysis of  $T_g(r)$  indicated that the  
 515 early part of the curve is sensitive to the variance of the  $T$  field while the rate at which it  
 516 approaches the geometric mean of  $T$  in the full domain could be related to the integral scale.  
 517 This provided the basis for attempting to use  $T_g(r)$  for estimating  $V$  and  $I$ .

518 The estimation of  $V$  and  $I$  was formulated using a Bayesian approach which expresses the  
 519 conditional pdf of  $V$  and  $I$  as a weighted function of the prior pdf and the likelihood function  
 520 that is itself dependent on the pumping test data. An important advantage of this approach is  
 521 that the likelihood function is readily computed from multiple realizations of the  
 522 transmissivity without the need to solve potentially complex inverse problems. Another  
 523 feature of the Bayesian approach is that it provides a measure of the uncertainty of the  
 524 estimated statistical parameters.

525 The Bayesian estimation procedure was applied to a number of synthetic pumping tests. The  
 526 analysis assumed that the natural log transform of the transmissivity distribution is a  
 527 multivariate Gaussian random spatial function with an exponential variogram. The variance  
 528 and integral scale were assumed to have a uniform joint prior distribution. The diffuse prior  
 529 distributions considered in this application and the non-uniqueness of the likelihood function  
 530 means that the results of the estimation procedure can be associated with a significant level  
 531 of uncertainty, highlighting the challenges of the parameter estimation problem. Single as  
 532 well as multiple pumping tests ( $N=5$  and  $N=10$ ) were assumed to be available. In the case  
 533 when multiple pumping tests were available, it was further assumed that they are located far  
 534 from each other such they sample different portions of the aquifer.

535 The significance of the Bayesian estimation procedure becomes apparent when the  
 536 conditional distribution of  $V$  and  $I$  is compared to the prior pdf of  $V$  and  $I$  which represents  
 537 the level of information available prior to conducting the pumping tests. It is shown that  
 538 improved estimates of  $V$  and  $I$  are obtained as the number of available pumping tests  
 539 increases or when more accurate prior distributions are available. The results of this  
 540 numerical example show that as little as 5 pumping tests may be sufficient to yield reliable  
 541 estimates of the statistical parameters of the transmissivity field.

Overall, the proposed interpretation procedure can be viewed as an extension of traditional pumping test interpretation procedures, such as the Theis method, that besides best-fit estimates of the storativity and transmissivity, can potentially also provide estimates of the variance and integral scale of the transmissivity field.

## 5. Acknowledgements

Mehmet Taner Demir and Nadim Coptly acknowledge the financial support provided by the Bogazici University Research Fund (BAP), Istanbul, Turkey (Project Number 6722).

Xavier Sanchez-Vila acknowledges support from the ICREA Academia Program. This paper has benefited from helpful comments by Walter Illman and two anonymous reviewers.

## 6. References

- Attinger, S., 2003. Generalized Coarse Graining Procedures for Flow in Porous Media, *Computational Geosciences*, 7(4), 253-273,
- Avci, C.B., Sahin, A.U., Ciftci, E., 2011. Aquifer Parameter Estimation Using an Incremental Area Method, *Hydrological Processes*, 25(16), 2584–2596.
- Avci, C.B., Sahin, A.U., Ciftci, E., 2013. A new method for aquifer system identification and parameter estimation, *Hydrological Processes*, 27(17), 2485–2497.
- Avci, C. B., Sahin, A.U., 2014. Assessing radial transmissivity variation in heterogeneous aquifers using analytical techniques, *Hydrological Processes*, 28, 5739–5754.
- Barker, J.A., Herbert, R., 1982. Pumping tests in patchy aquifers. *Ground Water*, 20, 150–155.
- Binley, A., Hubbard, S.S., Huisman, J.A., Revil, A., Robinson, D.A., Singha, K., Slater, L.D., 2015. The emergence of hydrogeophysics for improved understanding of subsurface processes over multiple scales, *Water Resour. Res.*, 51, 3837–3866, doi:10.1002/2015WR017016.
- Bohling, G.C., and Butler Jr., J.J., 2010. Inherent limitations of hydraulic tomography. *Ground Water* 48(6), 809–824.



- 570 Bohling, G.C., Liu, G., Knobbe, S.J., Reboulet, E.C., Hyndman, D.W., Dietrich, P., Butler,  
571 J.J., 2012. Geostatistical analysis of centimeter-scale hydraulic conductivity  
572 variations at the MADE site, *Water Resour. Res.*, 48, W02525,  
573 doi:10.1029/2011WR010791.
- 574 Bourdet, D., 2002. *Well Test Analysis: The Use of Advanced Interpretation Models*, Elsevier,  
575 Amsterdam, Boston.
- 576 Butler Jr., J.J., 1988. Pumping tests in nonuniform aquifers - The radially symmetric case.  
577 *Journal of Hydrology*, 101, 15–30.
- 578 Butler Jr., J.J. 1990. The role of pumping tests in site characterization: some theoretical  
579 considerations, *Ground Water*, 28(3), 394-402.
- 580 Butler Jr., J.J., McElwee, C.D., Bohling G. C. 1999. Pumping tests in networks of multilevel  
581 sampling wells: Motivation and methodology, *Water Resour. Res.*, 35(11), 3553-  
582 3560, doi:10.1029/1999WR900231.
- 583 Butler Jr., J.J., Dietrich, P., Wittig, V., Christy T., 2007. Characterizing hydraulic  
584 conductivity with the direct-push permeameter, *Ground Water*, 45(4), 409-419.
- 585 Cooper, H., Jacob C., 1946. A generalized graphical method for evaluating formation  
586 constants and summarizing well-field history, *Trans., Am. Geophys. Union*, 27(4),  
587 526-534.
- 588 Coptý, N.K., Findikakis A.N., 2004a. Stochastic analysis of pumping test drawdown data in  
589 heterogeneous geologic formations, *J. Hydraul. Res.*, 42, 59-67.
- 590 Coptý, N.K., Findikakis A.N., 2004b. Bayesian identification of the local transmissivity  
591 using time-drawdown data from pumping tests, *Water Resour. Res.*, 40, W12408,  
592 doi:10.1029/2004WR003354.
- 593 Coptý, N.K., Trinchero, P., Sarioglu, M.S., Findikakis, A.N., Sanchez-Vila, X., 2008.  
594 Influence of heterogeneity on the interpretation of pumping test data in leaky  
595 aquifers, *Water Resour. Res.*, 44, W11419, doi:10.1029/2008WR007120
- 596 Coptý, N.K., Trinchero, P., Sanchez-Vila, X., 2011. Inferring spatial distribution of the  
597 radially integrated transmissivity from pumping tests in heterogeneous confined  
598 aquifers, *Water Resour. Res.*, 47 (5). W05526, doi:10.1029/2010WR009877.

- 599 Delay, F., Ackerer, P., Belfort, B., Guadagnini, A., 2012. On the emergence of reciprocity  
600 gaps during interference pumping tests in unconfined aquifers, *Adv. Water Resour.*,  
601 46, 11–19, doi:10.1016/j.advwatres.2012.06.002.
- 602 Dietrich P., Butler, J.J. Jr, Faiss, K., 2008. A rapid method for hydraulic profiling in  
603 unconsolidated formations, *Ground Water*, 46(2), 323-328.
- 604 Feitosa, G.S., Chu L., Thompson, L.G., Reynolds, A.C., 1994. Determination of  
605 permeability distribution from well test pressure data. *Society of Petroleum*  
606 *Engineers*, 26: 407.
- 607 Firmani, G., Fiori, A., Bellin, A., 2006. Three-dimensional numerical analysis of steady state  
608 pumping tests in heterogeneous confined aquifers, *Water Resour. Res.*, 42, W03422,  
609 doi:10.1029/2005WR004382
- 610 Gelhar, L.W., 1993. *Stochastic Subsurface Hydrology*, Prentice-Hill, 643 Upper Saddle  
611 River, N. J.
- 612 Harbaugh, A.H., Banta, E.R., Hill, M.C., McDonald, M.G., 2000. MODFLOW-2000, The  
613 U.S. Geological Survey Modular Ground-Water Model- User Guide to  
614 Modularization Concepts and the Ground-Water Flow Process, U.S. Geological  
615 Survey, Open-File Report 00-92.
- 616 Illman, W.A., Berg, S.J., Zhao Z., 2015. Should hydraulic tomography data be interpreted  
617 using geostatistical inverse modeling? A laboratory sandbox investigation, *Water*  
618 *Resour. Res.*, 51, doi:10.1002/ 2014WR016552
- 619 Kitanidis, P.K., 1997. *Introduction to Geostatistics: With Applications in Hydrogeology*,  
620 Cambridge University Press, New York.
- 621 Knight, J., Kluitenberg, G., 2005. Some analytical solutions for sensitivity of well tests to  
622 variations in storativity and transmissivity, *Adv. in Water Res.*, 28 (10), 1057-1075,
- 623 Leven, C., Dietrich, P., 2006. What information can we get from pumping tests? comparing  
624 pumping test configurations using sensitivity coefficients, *J. Hydrol.*, 319 (14), 199-  
625 215.
- 626 Mantoglou, A., Wilson J.L, 1982. The turning bands method for simulation of random-fields  
627 using line generation by a spectral method, *Water Resour. Res.*, 18(5), 1379-1394.
- 628 Meier, P.M., Carrera, J., Sanchez-Vila, X., 1998. An evaluation of Jacob's method for the  
629 interpretation of pumping tests in heterogeneous formations, *Water Resour. Res.*,  
630 34(5), 1011-1025.

- 631 Neuman, S.P., Guadagnini, A., Riva, M., 2004. Type-curve estimation of statistical  
632 heterogeneity, *Water Resour. Res.*, 40, W04201, doi:10.1029/2003WR002405.
- 633 Neuman, S.P., Blattstein, A., Riva, M., Tartakovsky, D.M., Guadagnini, A., Ptak, T., 2007.  
634 Type curve interpretation of late-time pumping test data in randomly heterogeneous  
635 aquifers, *Water Resour. Res.*, 43, W10421, doi:10.1029/2007WR005871
- 636 Oliver, D.S. 1993. The influence of nonuniform transmissivity and storativity on drawdown,  
637 *Water Resour. Res.*, 29(1), 169-178, 1993.
- 638 Pechstein, A., Attinger, S., Krieg, R., Copt, N.K., 2016. Estimating transmissivity from  
639 single-well pumping tests in heterogeneous aquifers, *Water Resour. Res.*, 52(1), 495-  
640 510
- 641 Renard, P., 2007. Stochastic hydrogeology: what professionals really need? *Ground Water*,  
642 45, 531-541.
- 643 Riva, M., Guadagnini, A., Bodin, J., Delay, J., 2009. Characterization of the hydrogeological  
644 experimental site of Poitiers (France) by stochastic well testing analysis, *J. Hydrol.*,  
645 369(1-2), 154-164.
- 646 Rubin, Y., 2003. *Applied Stochastic Hydrogeology*, Oxford University Press. New York.
- 647 Rubin, Y., Hubbard, S., 2005. *Hydrogeophysics*, Series: Water Science and Technology  
648 Library, 50, Springer.
- 649 Sanchez-Vila, X., Ackerer, P., Delay, F., Guadagnini, A., 2016. Characterization of  
650 reciprocity gaps from interference tests in fractured media through a dual porosity  
651 model, *Water Resour. Res.*, 52, doi:10.1002/2015WR018171.
- 652 Sanchez-Vila, X., Fernández-García, D., 2016. Debates-Stochastic subsurface hydrology  
653 from theory to practice: Why stochastic modeling has not yet permeated into  
654 practitioners?, *Water Resour. Res.*, 52, 9246–9258, doi:10.1002/2016WR019302.
- 655 Sanchez-Vila, X., Guadagnini, A., Carrera, J., 2006. Representative hydraulic conductivities  
656 in saturated groundwater flow, *Rev. Geophys.*, 44(3), RG3002.
- 657 Sanchez-Vila, X., Meier, P.M., Carrera, J., 1999. Pumping tests in heterogeneous aquifers:  
658 An analytical study of what can be obtained from their interpretation using Jacob's  
659 method, *Water Resour. Res.*, 35(4), 943–952.
- 660 Slater, S., 2007. Near surface electrical characterization of hydraulic conductivity: from  
661 petrophysical properties to aquifer geometries—A review, *Surv Geophys* 28, 169–  
662 197, doi:10.1007/s10712-007-9022-y

- 663 Sudicky, E.A., Illman, W.A., Goltz, I.K., Adams, J.J., McLaren, R.G., 2010. Heterogeneity  
 664 in hydraulic conductivity and its role on the macroscale transport of a solute plume:  
 665 From measurements to a practical application of stochastic flow and transport theory,  
 666 *Water Resour. Res.*, 46, W01508, doi:10.1029/2008WR007558.
- 667 Tarantola, A., 1987. *Inverse Problem Theory, Methods for Data Fitting and Model*  
 668 *Parameter Estimation*, Elsevier Science Publishers, Amsterdam, Holland.
- 669 Theis, C.V., 1935. The relation between the lowering of the piezometric surface and the rate  
 670 and duration of discharge of a well using groundwater storage, *Trans., Am. Geophys.*  
 671 *Union*, 16, 519– 524.
- 672 Trinchero, P., Sanchez-Vila, X., Coptý, N.K., Findikakis, A.N., 2008a. A new method to  
 673 interpret pumping tests in leaky aquifers, *Ground Water*, 46(1), 133-143.
- 674 Trinchero, P., Sanchez-Vila, X., Fernandez-Garcia, D., 2008b. Point-to-point connectivity,  
 675 an abstract concept or a key issue for risk assessment studies?, *Adv. Water Resour.*,  
 676 31(12), 1742-1753.
- 677 Yeh, T.C.J., Liu, S., 2000. Hydraulic tomography: Development of a new aquifer test  
 678 method, *Water Resour. Res.*, 36(8), 2095– 2105.
- 679 Yin, D. T., Illman, W.A., 2009. Hydraulic tomography using temporal moments of  
 680 drawdown recovery data: A laboratory sandbox study, *Water Resour. Res.*, 45, Art.  
 681 No. W01502.
- 682 Zech, A., Schneider, C.L., Attinger, S., 2012. The Extended Thiem's solution: Including the  
 683 impact of heterogeneity, *Water Resour. Res.*, 48 (10), W10,535.
- 684 Zech, A., Arnold, S., Schneider, C.,L., Attinger, S., 2015. Estimating Parameters of Aquifer  
 685 Heterogeneity Using Pumping Tests - Implications for Field Applications, *Adv.*  
 686 *Water Resour.*, 83,137–147.
- 687 Zech, A., Müller, S., Mai, J., Heße, F., Attinger S., 2016. Extending Theis' solution: Using  
 688 transient pumping tests to estimate parameters of aquifer heterogeneity, *Water*  
 689 *Resour. Res.*, 52, 6156–6170, doi:10.1002/2015WR018509.
- 690 Zhu, J., Yeh, T.J., 2005. Characterization of aquifer heterogeneity using transient hydraulic  
 691 tomography, *Water Resour. Res.*, 41, W07028, doi:10.1029/2004WR003790.